Journal of Quaternary Science

A late glacial – Holocene record of hydrological variability in Lake Baikal inferred from oxygen isotope analysis of diatom silica

Journal:	*Journal of Quaternary Science*
Manuscript ID:	JQS-10-0094
Wiley - Manuscript type:	Research Article
Date Submitted by the Author:	22-Jun-2010
Complete List of Authors:	Mackay, Anson; UCL, Geography Swann, George; NERC Isotope Geosciences Laboratory Brewer, Tim; University of Leicester, Department of Geology Leng, Melanie; NERC Isotope Geosciences Laboratory Morley, David; UCL, Department of Geography Piotrowska, Natalia; Silesian University of Technology, Department of Radioisotopes Rioual, Patrick; Chinese Academy of Science, Geology and Geophysics Institute White, Dustin; University of Oxford, Institute of Archaeology
Keywords:	Lake Baikal, δ18Odiatom, late glacial, Holocene, IRD events

A late glacial – Holocene record of hydrological variability in Lake Baikal inferred from oxygen isotope analysis of diatom silica.

Anson W. Mackay[a,1]
[a]Environmental Change Research Centre, Department of Geography, UCL, Gower Street London. United Kingdom. WC1E 6BT.
Email: a.mackay@ucl.ac.uk
[1]Corresponding author

George E.A. Swann[b]
[b]NERC Isotope Geosciences Laboratory, British Geological Survey, Keyworth, Nottingham, NG12 5GG, UK

Tim S. Brewer[c,2]
[c]Department of Geology, University of Leicester, Leicester, United Kingdom. LE1 7RH.
[2]Deceased

Melanie J. Leng[b,d]
[b]NERC Isotope Geosciences Laboratory, British Geological Survey, Keyworth, Nottingham, NG12 5GG, UK
[c]School of Geography, University of Nottingham, Nottingham, United Kingdom. NG7 2RD

David W. Morley[a,e]
[a]Environmental Change Research Centre, Department of Geography, UCL, Gower Street London. WC1E 6BT
[e] Spatial Ecology and Epidemiology Group, Department of Zoology, South Parks Road, University of Oxford, Oxford, United Kingdom. OX1 3PS

Natalia Piotrowska[f]
[f]Silesian University of Technology, Institute of Physics, Department of Radioisotopes, GADAM Centre of Excellence, Krzywoustego 2, 44-100 Gliwice, Poland

Patrick Rioual[g]
[g]Geology and Geophysics Institute, Chinese Academy of Science, P.O. Box 9825, Beijing 100029, China

Dustin White[h]
[h]Institute of Archaeology, University of Oxford, 36 Beaumont Street, Oxford, United Kingdom. OX1 2PG.

Abstract

Here we present a new palaeoenvironmental record of hydrological variability in Lake Baikal since c. 14 100 cal yrs BP, based on re-modelled $\delta^{18}O_{diatom}$ values of diatom silica ($\delta^{18}O_{modelled}$), where the residual contaminants are identified and compensated for using electron optical imaging and whole sample geochemistry. $\delta^{18}O_{modelled}$ interpretations are based on the balance between isotopically higher rivers, which have catchments to the south of Lake Baikal, and isotopically lower rivers with catchments to the north. Isotopic differences are due to varying proportions of precipitation and snow-melt which feed these rivers. The balance between northern and southern rivers flowing into Lake Baikal is mediated by the strength of the Siberian High. Overall, episodic declines in $\delta^{18}O_{modelled}$ values show good agreement with increases in %HSG grains in the North Atlantic (indicative of ice-rafted debris events). Periods when the contribution of isotopically lower rivers with northern catchments increases are coincident with increases with IRD events at e.g. c. 11 300 cal yr BP (IRD8), c. 10 200 cal yr BP (IRD7), c. 8 400 cal yrs BP (IRD5), c. 7 000 cal yrs BP, c. 5 900 cal yrs BP (IRD4) and 3 330 cal yrs BP (IRD2). Isotopically higher input from rivers to the south Lake Baikal is especially dominant between c. 3 300 – 2 000 cal yrs BP, concurrent with high precipitation amounts in the Lake Baikal region and northern Mongolia. This study highlights the potential for oxygen isotope analysis of diatom silica to reconstruct the past hydrology of Lake Baikal, and its possible relationship with distant events such as changes in the North Atlantic thermohaline circulation.

Keywords: Lake Baikal; $\delta^{18}O_{diatom}$; late glacial; Holocene; IRD events

1. Introduction

Lake Baikal (51°28' - 55°47' N and 103°43' - 109°58' E) in central Asia is situated in one of the most continental regions of Earth, where climate is strongly influenced the Siberian High, a high pressure cell which starts to build in strength in August, and remains strong until the following April. Precipitation to the Lake Baikal region mainly originates from the North Atlantic and is transported via the Westerlies (Lydolph 1977; Numaguti 1999; Kurita et al. 2004), with very little contribution from tropical sources (Sato et al. 2007). Precipitation throughout the Lake Baikal region is greatest during June, July and August (JJA) (Kozhova & Izmest'eva 1998). Winters on the other hand are dominated by the Siberian High, which ensures that winters are cold, dry and long (Lydolph 1977). Lake Baikal contains approximately one fifth of the world's global resources of surface freshwater, and species living in the lake exhibit high levels of endemicity (Kozhova & Izmest'eva 1998). Given recent debates on threats to freshwater resources and biodiversity, understanding the functioning of such a complex ecosystem remains an important research priority. Climate is a major driver of ecosystem change, and studies have demonstrated the impacts of recent warming on both the ice cover of Lake Baikal (e.g. Livingstone 1999; Todd & Mackay 2003) and on its biology (Mackay et al. 2005; Hampton et al. 2008). To gain a wider perspective on these changes, it is important to study hydrological trends in Lake Baikal over longer timescales.

For example, during the late glacial, one of the most distinctive shifts in climate was the period commonly known as the Younger Dryas (GS-1), c. 12 900 cal yrs BP. This abrupt cold reversal in the North Atlantic region is linked to an enormous pulse of freshwater being released from the Laurentide ice sheet into the Arctic Ocean (Tarasov and Peltier 2005; Murton et al., 2010), causing a decline in global temperatures (as inferred from $\delta^{18}O$ records from the Greenland ice cores). During the Holocene, centennial-scale cool events (Bond events (Bond et al. 1997)) have been identified in natural archives from around the world (e.g. Campbell et al. 1998; deMenocal et al. 2000; Heiri et al. 2004; Mayewski et al. 2004; Nesje et al. 2005; Wanner et al. 2008). These events are associated with pulses of freshwater discharge from the Laurentide ice sheet weakening North Atlantic thermohaline circulation (THC), resulting in the southwards extension of polar waters (Bond et al. 1997). Changes in solar insolation are also implicated (e.g. Bond et al. 2001), whilst after c. 8 000 cal yrs BP these events are likely due to a combination of other factors (Wanner et al. 2008).

In dilute, lacustrine systems where preservation of carbonates is poor (such as Lake Baikal), oxygen isotope analysis of diatom silica ($\delta^{18}O_{diatom}$) is potentially an important palaeoclimatic technique that can be used as a direct replacement for $\delta^{18}O$ from carbonates. For example, during the last glacial – interglacial transition in southwest Alaska, a decline in $\delta^{18}O_{diatom}$ values at the start of the Younger Dryas was interpreted as being caused by a drop in temperature of over 3.5 ºC (Hu & Shemesh 2003). In Lake 850, close to Abisko in the Swedish Arctic, $\delta^{18}O_{diatom}$ values are thought to reflect varying sources of precipitation to the region, such that a persistent decline in $\delta^{18}O_{diatom}$ during the Holocene is linked to increasing influence of the polar Arctic continental air mass (Shemesh et al. 2001). Through $\delta^{18}O_{diatom}$ analyses of lake sediments from the Kola Peninsula, polar Arctic air masses were also shown to dominate this region of northwest Russia during the early and late Holocene, while during the mid Holocene maritime Atlantic air masses were important (Jones et al. 2004). In a further study of a proglacial lake in the Swedish Arctic, Rosqvist et al. (2004) demonstrate a clear correlation between periods of glacier advancement and $\delta^{18}O_{diatom}$ minima during the late Holocene linked to increased influence of polar air masses. These minima occur at approximately the same time as Bond events, confirming the increased influence of N-NE winds in this region of the north Atlantic (Rosqvist et al. 2004).

$\delta^{18}O_{diatom}$ analyses have previously been used to reconstruct environmental change in Lake Baikal during the late glacial (Morley et al. 2005), MIS 3-1 (Kalmychkov et al., 2007) and during MIS 11 (Mackay et al. 2008). In Lake Baikal, changes in $\delta^{18}O_{diatom}$ values have been linked to variation in fluvial input, most notably between rivers with catchments which extend to the south of Lake Baikal into Mongolia, with rivers with more northerly catchments (Fig 1). Changes in air temperature have been considered, but given that rainfall water–temperature fractionation is +0.36‰/°C (the Dansgaard temperature dependence in precipitation at Irkutsk), shifts in isotopic values observed in Lake Baikal records are too great to have been caused by temperature alone (Seal and Shanks 1998; Morley et al. 2005). Over 330 rivers flow into Lake Baikal, the most significant being the Selenga, Upper Angara and Barguzin Rivers contributing c. 50%, 14% and 7% of total annual river inflow respectively (Shimaraev et al. 1994) (Fig. 1).

The Selenga River therefore is by far the most important river in terms of hydrological input into Lake Baikal. Just under half of Lake Baikal's catchment belongs to the Selenga River basin, c. 280,000 km^2, which drains much of northern Mongolia between 46-52° N and 96-109° E (Fig. 1) (Ma et al. 2003). Any changes in its flow therefore will result in hydrological changes in the lake itself.

Lake Baikal contains three large basins (north, central, south) and the form of moisture contributing to river flow to these basins varies considerably. For example, snow-derived water accounts for just under one third of total fluvial input into the north basin. The Selenga River on the other hand, which drains into the south and central basins, consists of only c. 15% snow-derived water (Afanasjev 1976). Conversely, the proportion of water derived from rainfall is highest in the Selenga River (almost 40%), whereas for rivers that flow into the north basin, this proportion drops to only c. 20%. These contribute to the variation in isotope values of modern waters which show that rivers with catchments to the south of Lake Baikal are characterized by higher $\delta^{18}O$ values (e.g. –13.5‰ for the Selenga River), in comparison to rivers with more northern catchments (e.g. the Barguzin and Upper Angara Rivers) with lower $\delta^{18}O$ values (–17.3‰ and –19.8‰ respectively; Seal and Shanks 1998). During periods of cooler temperatures and prolonged winters, instrumental and remotely sensed data show that increased Eurasian spring snow cover extent results in a reduction in summer precipitation (especially over the Selenga catchment) through increased anticyclonic activity and strength of the Siberian High (Lui & Yanai 2002). Thus rivers with higher $\delta^{18}O$ values to the south of Lake Baikal decline in volume, while northern rivers fed by a higher proportion of snowmelt increase (Morley et al. 2005). Previous work investigating trends in ice cover on Lake Baikal has shown significant links with northern annular modes (especially the North Atlantic Oscillation and Arctic Oscillation; Livingstone 1999; Todd & Mackay 2003). It is possible that these modes are also having an impact on transport of moisture to the Lake Baikal region via the Westerlies.

Demske et al. (2005) suggested that there is distinct pollen evidence for climatic impact in the Lake Baikal region related to Holocene cool events in the North Atlantic (Bond et al. 1997). A major aim of this paper therefore, is to assess any potential impact of such cool events on hydrological inflow into Lake Baikal. In order to do this, we present a new $\delta^{18}O_{diatom}$ record derived from the recalculation of data first published by Morley et al. (2005). This recalculation is necessary due to recent advances in the application of whole sample geochemistry coupled with electron-optical imaging in providing a method for the identification, estimation and subsequent removal of the effects of clay and silt contamination on $\delta^{18}O_{diatom}$ data (Brewer et al. 2008). Due to issues of contamination on the $\delta^{18}O_{diatom}$ record by silts and clays, palaeo-environmental interpretations of the Holocene were barely made by Morley et al. (2005). We also take advantage of IntCal04 calibration curve over IntCal98, which provides much improved calibrated dates for samples deposited prior to 11 400 cal yrs BP, a key timeframe in our analyses (Blackwell et al. 2006).

3. Materials and methods

3.1 Site location and coring

The Vydrino Shoulder (51.58°N, 104.85°E) is located off the southeastern coast of Lake Baikal (c. 5 km) between 500 – 800 m water depth (Fig. 1). Given its proximity to the shore, Vydrino is also likely influenced by fluvial input from nearby rivers, including the Snezhnaya and Vydrinaya. The Shoulder forms an upper- to mid-slope terrace dissected by several canyons (Charlet et al. 2005) and is in the vicinity of several underwater channels. In the summer of 2001, different core types of varying length were extracted from a ridge location (>600 m water depth) on the Vydrino Shoulder. Of relevance to this study, these include a long piston core over 10 m in length and a separate box core of c. 2.5 m in length (Table 1). This ridge was selected because seismic profiling and side-scan sonar analyses revealed a stable area of fine-grained sedimentation relatively undisturbed by tectonic activity and reworking (Fig. 3 in Charlet et al. 2005).

3.2 Chronology

Plant macrofossils are rarely preserved in the pelagic sediments of Lake Baikal, so AMS ^{14}C dates were obtained from pollen and spore concentrates (Piotrowska et al. 2004; Demske et al. 2005). The late glacial – Holocene age model for Vydrino Shoulder is based upon twelve AMS ^{14}C pollen dates from the box core (CON01-605-5) (Piotrowska et al. 2004) and an additional five AMS ^{14}C pollen dates from the piston core (CON01-605-3) (Demske et al. 2005). Pollen purity was excellent (80% – 95%) in each box-core sample due to the presence of very high concentrations of large bisaccate pollen grains (Table 2); unfortunately purity data for the pollen extracts obtained from the piston cores are not available, which indirectly adds to uncertainty of dates obtained for pre-Holocene sediments. Dates from the box core were transferred to the piston core based on easily identified peaks in relative abundances of specific diatom species common to both cores, including a well defined peak of *Hannaea baicalensis* Genkal, Popovskaya, Kulikovskiy during the early Holocene, and a mid Holocene switch between *Crateriportula inconspicua* and *Synedra acus* (Kützing) (data not shown - see Morley 2005 and Morley et al. 2005). All radiocarbon dates were calibrated using OxCal 4.1 program (Bronk Ramsey 2009) and IntCal04 radiocarbon calibration curve (Reimer et al. 2004) (Table 2). To estimate a relationship between age and depth we used a generalised mixed-effect regression based on a generalised additive model (GAM) with constant variance (Heegaard et al. 2005).

3.3 $\delta^{18}O_{diatom}$ analysis

Samples for $\delta^{18}O_{diatom}$ came from the piston core (CON01-605-3). Sediments were originally analysed for $\delta^{18}O_{diatom}$ at contiguous 2 cm intervals by Morley et al. (2005), although a reduced dataset is presented here. The methodology for cleaning samples for $\delta^{18}O_{diatom}$ analysis has previously been reported by Morley et al. (2004), and involves the step-wise removal of contaminants using chemical and physical separation techniques. Cleaned, dried samples were first subjected to a prefluorination process to remove the unstable hydrous silica layer from the diatom valves, before full reaction with BrF_5 (Leng and Sloane, 2008). Liberated oxygen was converted to CO_2 and measured alongside BFC_{mod} the NIGL diatom standard with $\delta^{18}O$ analysis performed using an Optima dual inlet mass spectrometer. The data are presented as per mil (‰) deviations from SMOW with replicate analysis of sample material indicating an analytical reproducibility of ±0.34‰ (1 σ).

Subsequent SEM analyses of these cleaned samples demonstrated that a small but significant proportion of contaminants remained after sample preparation. These contaminants were comprised of clay and silt material trapped, for example, within the cylindrical frustules of *Aulacoseira* species or as clay particles coated with sub-micron scale diatom fragments (Brewer et al. 2008). Morley et al. (2005) tried to compensate for these remaining contaminants by calculating the $\delta^{18}O$ value of the non-diatom particles as an average of clay and silt sized mineral/rock grains (called 'silt') remaining in the sample following the removal of diatoms with sodium hydroxide (12.3 ± 1.8‰, 2 S.D., n=3). A mass balanced $\delta^{18}O$ value for pure diatoms ($\delta^{18}O_{modelled}$) was therefore calculated using the estimated percentage content of diatoms and silt identified using light microscopy for individual samples. This methodology however underestimates the effect of silt $\delta^{18}O$ because volumes of diatoms and silt particles are not taken into account (Leng and Barker 2006), resulting in a significant uncertainty in the original $\delta^{18}O_{modelled}$ data. Due to this, an interpretation of the Holocene $\delta^{18}O_{diatom}$ and $\delta^{18}O_{modelled}$ record was barely made (Morley et al. 2005).

This study differs significantly from Morley et al. (2005) because we use a mass-balance approach where the residual contaminants are identified and compensated for, using electron optical imaging and whole sample geochemistry (see Brewer et al. 2008 for full methodological details). Note however, that only 55 of the 130 samples analysed by Morley et al., (2005) contained sufficient quantities of diatoms for XRF analysis, resulting in a substantial reduction in sample resolution. Under the geochemical mass balancing approach, the relative amount of silt contamination can be calculated from the amount of Al_2O_3 in individual samples. Brewer et al., (2008) achieved this by:

$$\%silt = (sample_{Al}/silt_{Al}) \times 100 \qquad (1)$$

where $sample_{Al}$ is the measured Al_2O_3 concentration in each sample analysed for $\delta^{18}O_{diatom}$ and $silt_{Al}$ the average $\%Al_2O_3$ in the Baikal silt sample, calculated in Brewer et al (2008) as 16.8%.

A key assumption of this is that concentrations of Al within diatoms are negligible. A number of studies, however, have shown that fossilised diatoms can contain up to 1 wt.% Al (see Koning et al. (2007) and references within). Recent work on fully purified MIS 5e diatom samples from Lake Baikal shows Al concentrations of 0.08% [$1\sigma = 0.02$]) (Swann in press). Although this level of diatom bound Al typically only alters modelled $\delta^{18}O_{diatom}$ within the limits of analytical reproducibility (0.34‰) it nevertheless remains important to account for this contribution. By assuming that Al concentrations in MIS 5e diatoms from Lake Baikal are representative of the late glacial – Holocene aged diatoms analysed here, a separate initial mass balance calculation can be performed to distinguish between diatom Al/silt Al and so calculate %diatom and %silt:

$$sample_{Al} = (\%diatom \bullet diatom_{Al}) + (\%silt \bullet silt_{Al}) = (\%diatom \bullet 0.15) + (\%silt \bullet 17.2\%) \qquad (2)$$

where $diatom_{Al}$ is the %Al in diatom converted into $\%Al_2O_3$, %diatom and %silt the percent diatom and silt within the analysed sample and $silt_{Al}$ is the corresponding value from Brewer et al (2008) re-normalised following the removal of LOI data which constitutes water and other organic matter that will be removed during the pre-fluorination stage of the $\delta^{18}O_{diatom}$ analysis. A further mass balance correction is then employed to account for the effects of silt contamination on the measured $\delta^{18}O$ values:

$$\delta^{18}O_{modelled} = (\delta^{18}O_{diatom} - \%silt_O/100 \times \delta^{18}O_{silt})/(\%diatom_O/100) \qquad (3)$$

where $\delta^{18}O_{modelled}$ is the mass balance corrected value of $\delta^{18}O_{diatom}$, $\delta^{18}O_{diatom}$ is the original isotope value of the "cleaned" diatom sample, $\delta^{18}O_{silt}$ is the average isotope value of silt from Lake Baikal, measured at 11.7 ± 0.3‰ (n=6) in Brewer et al. (2008), and $\%diatom_O/\%silt_O$ is the percentage of diatom and silt with respect to oxygen. $\%silt_O$ is calculated by assuming that 48.6 wt.% of the contaminant silt is comprised of oxygen (c.f., Brewer et al., 2008) whilst for $\%diatom_O$ we assume that diatoms are comprised of SiO_2 with oxygen making up 53.3% of the diatom frustule. An estimate of the error associated with this mass balance correction can be obtained for each sample by factoring in an analytical reproducibility of 0.34‰ for both the diatom and Baikal silt isotope measurements into equation 3.

4. Results and Discussion

The calibrated ages for our profile span approximately the last 15 700 cal yrs BP (range 15 275 – 16 090 cal yrs BP) (Fig 2). The age-depth curve was determined using mixed-effect regression (Heegaard et al. 2005). The calculations of model confidence intervals take into consideration not only the width of probability distribution of calibrated ages, but also the representativity of individual dates for the sequence. The average 95% confidence intervals for most of the profile (13 000 – 2 000 cal yrs BP) range from ±120 to ±200 years. For the younger part, the confidence intervals increase from ±35 to ±150 years, while for the ages older than 13 000 cal yrs BP they continuously rise from ±200 to almost ±400 years. As the thickness of the sediment samples used for dating is taken into account, this results in the wider confidence intervals observed during the late glacial, early Holocene period (see Table 2). The model also reveals that the top-most radiocarbon date is not close to the expected value, and therefore probably poorly represents the real age of this layer (Heegaard et al. 2005). Given this chronology, the resolution of the $\delta^{18}O_{modelled}$ profile varies between c. 375 – 400 years. Using the IntCal04 calibration curve, the timing of $\delta^{18}O_{modelled}$ changes during the early part of our record have changed substantially from that first presented by Morley et al. (2005) by c. 1000 years. For example, the low $\delta^{18}O_{diatom}$ value reported by Morley et al. (2005) at c. 11 300 cal yrs BP is estimated now to occur at c. 10 300 cal yrs BP, which is a direct result of the improved calibration curve during this key period (Blackwell et al 2006).

Robust interpretations of $\delta^{18}O_{diatom}$ data from lake sediments are reliant on intensive cleaning and mass balance modelling procedures for removing effects of contaminants. Brewer et al. (2008) showed that Baikal silt is enriched in Al_2O_3, Fe_2O_3, Na_2O and K_2O, such that the incorporation of silt within diatom samples should be clearly identifiable through their trace element geochemistry. Using sample Al_2O_3 concentrations as an estimator of contamination, the amount of non-diatom material within the Vydrino samples ranges from <10% to c. 90%. This highlights that the purification method described by Morley et al. (2004) can be inefficient. The presence of non-diatom contaminants in samples analysed for $\delta^{18}O_{diatom}$ or other diatom isotopes/geochemical analyses is not restricted to Lake Baikal. Regardless of the adopted procedure, the majority of lacustrine and marine samples will contain a proportion of clays, silts, or other siliceous material such as sponges or phytoliths after sample cleaning (Leng and Barker, 2006; Lamb et al., 2007; Swann and Leng, 2009). Indeed some samples are impossible to fully purify due to contaminants becoming electro-statically charged to frustules (Brewer et al, 2008). Despite this, in the majority of cases issues of contamination are not considered despite their potential to distort the isotope record. Increasing awareness of these issues and the development of more sophisticated methods for assessing levels of contamination are however beginning to resolve this issue (Swann and Leng, 2009). The mass balanced $\delta^{18}O_{modelled}$ data presented here therefore are a re-analysis of a subset of data previously presented by Morley et al. (2005), but with significant and important modifications. First, we are able to attribute error estimates to each modelled $\delta^{18}O$ value. Second, modelled $\delta^{18}O$ values have some of the high-frequency noise and some of the large low-frequency excursions removed (Fig 3). For example, mean $\delta^{18}O_{modelled}$ values are c. 5‰ higher using the mass-balance approach, with considerably smaller standard deviation (Table 3). Most striking is the influence of silt contamination on the records. The original record by Morley et al. (2005) is strongly influenced by the proportion of silt in the sample, such that as %silt increases, $\delta^{18}O_{diatom}$ values decline, in line with lower $\delta^{18}O$ value for silt. However, our $\delta^{18}O_{modelled}$ values exhibit a very different response with the contamination record; during the early Holocene, $\delta^{18}O_{modelled}$ values increase as silt contamination increases, and again to a lesser extent during the mid Holocene (Fig 3). Other potential confounding factors such as dissolution and vital effects for Lake Baikal diatoms are considered in detail in Mackay et al. (2008).

4.1 Palaeo-environmental interpretations

4.1.1 The late glacial period

The Bølling interstadial was the first period of warming after the last glacial, and is dated to approximately 14 600 – 14 100 cal yrs BP. $\delta^{18}O_{modelled}$ values are relatively high (c. +28‰) at this time, indicative of rivers such as the Selenga, with catchments to the south of Lake Baikal, dominating fluvial input. This is in line with a two-fold increase in precipitation, which resulted in increased catchment weathering around Lake Baikal, through increased river inflow and reduced aeolian transport (Chebykin et al. 2002). In the catchment, warming is associated with a marked expansion in shrub landscape, especially *Salix* species and *Alnus fruticosa* (Demske et al. 2005). Thus, although prevailing humidity and precipitation had increased, temperatures were still relatively cool, because *A. fruticosa* is characteristic of the sub-alpine mountain zone around Lake Baikal today. Two other diatom records from Lake Baikal also show moderate increases in diatom concentration during the Bølling period (Prokopenko et al. 2007). During the Allerød, the $\delta^{18}O_{modelled}$ record exhibits a low value of +25.3‰ at c. 13 450 cal yrs BP (Fig. 4), coincident with a decline in diatom concentration reported by Prokopenko et al. (2007) at c. 13 500 cal yrs BP. However, this decline in the isotope record is characterised by one point only, and future higher resolution work is needed to determine if this is a real shift in balance from rivers flowing into Lake Baikal from the south, to isotopically lower rivers flowing in from the north, associated with the timing of the onset of the intra-Allerød cold period (IACP) (e.g. Rasmussen et al. 2006).

The transition from the Allerød into the Younger Dryas is generally placed at c. 12 900 cal yrs BP. Proxy records in Lake Baikal are indicative of a decline in primary productivity with the onset of the Younger Dryas, although moisture records appear to be more complex. For example, a coarsely resolved biogenic silica record from BDP93 (Buguldeika Saddle) demonstrated a decline in diatom productivity linked to the Younger Dryas (Colman et al. 1999) while pigments such as total chlorophyll *a* from BDP93 also declined (Soma et al. 2007). Corresponding diatom concentrations from BDP93 also show a small reduction at this time, followed by a small increase at c. 12 000 cal yrs BP (Prokopenko et al. 2007). More recently, Watanabe et al. (2009) showed that between 12 800 – 11 600 cal yrs BP, mass accumulation rates of total organic carbon (MAR_{TOC}) on the Academician Ridge rapidly declined, indicative of falling productivity in the lake together with a decline in terrestrial organic material. At the start of the Younger Dryas $\delta^{18}O_{modelled}$ values initially decline to c. +26.9‰ indicative of only a small decline in river inflow into the south basin of Lake Baikal which persisted til c. 12 180 cal yrs BP. Pollen reconstructions show that by c. 12 500 cal yrs BP although temperatures dropped, low levels of evaporation maintained a rather humid climate (Tarasov et al. 2007). Pollen evidence elsewhere suggests that regions of peat formation around Lake Baikal started at the Allerød - Younger Dryas transition, again indicative that any decline in precipitation during the Younger Dryas was not enough to halt peat accumulation (Bezrukova et al. 2005). Further afield, detailed investigations on the palaeohydrology of Lake Hovsgol, which lies in the catchment of Lake Baikal, demonstrate that lake levels there started to increase irreversibly by about 15 400 cal yrs BP, which Prokopenko et al. (2005, 2009) suggest is due to increased precipitation in the southern catchment of Lake Baikal, before the start of the Holocene period. Further evidence for complex climate patterns during the Younger Dryas in this region of central Asia comes from Quaternary lake-level fluctuations of two northern Mongolian lakes (Bayan Nuur and Uvs Nuur) which exhibit high lake level stands from the Allerød through to the early Holocene, linked to melting glaciers and increased precipitation (Grunert et al. 2000). Increasing $\delta^{18}O_{modelled}$ values from c. 12 180 cal yrs BP suggest increased Westerly transport of precipitation to rivers to the south Lake Baikal, which must have been accompanied by a decline in intensity of the Siberian High. These findings are line with increasing pollen-inferred precipitation by c. 12 000 cal yrs BP elsewhere in the Lake Baikal region (Tarasov et al. 2009), and increasing global temperatures by c. 12 000 cal yrs BP (Stuiver et al. 1995). Overall, evidence from different proxies in the Lake Baikal region point to a period of reduced productivity but sustained effective moisture during the early stages of the Younger Dryas. By about 12 000 cal yrs BP however, hydrological inflow from isotopically higher rivers to the south of the lake increased again.

4.1.2 Early - mid Holocene (11 700 – 7 000 cal yrs BP)

We define the early Holocene as being the period when ice sheets were still a significant feature of northern hemisphere landscapes, modulating a climate which was principally being driven by orbital parameters. Relative summer insolation values at temperate latitudes (e.g. 53° N) were at their highest during the early Holocene, c. 10 000 cal yrs BP before gradually declining to the present day (Prokopenko et al. 2007). Average annual temperatures during the early Holocene were progressively getting warmer, although in central Asia, the difference between seasonal temperatures at temperate latitudes was very pronounced because of high obliquity resulting in relatively warm summers but very cold winters (Bush 2005). Here we show alongside the $\delta^{18}O_{modelled}$ values a stacked record of relative abundance of hematite stained grains (%HSG) which are a tracer of Holocene drift ice in the North Atlantic (Bond et al. 2001) (peaks are numbered according to Bond et al. 1997) (Fig 4). During this period, there are five distinct increases in %HSG in the North Atlantic.

At the start of this period, $\delta^{18}O_{modelled}$ values decline to +27.3‰ at c. 11 300 cal yrs BP, concomitant with a small decline in silt contamination (Fig 4). The decline in the $\delta^{18}O_{modelled}$ record is coincident with IRD8, commonly known as the Preboreal Oscillation (PBO), a cool event associated with freshwater discharge (possibly from Lake Agassiz) into the North Atlantic (Fisher et al. 2002). Through intensification of the Siberian High, this cool event is likely to have resulted in the relative decline in proportion of rain-fed rivers flowing into Lake Baikal and relative increase in isotopically-lower rivers flowing into the lake from the north. As above, we acknowledge that further work is needed to improve the resolution of the $\delta^{18}O_{modelled}$ signal at this time. However, pollen data from Vydrino also suggests a short period of cooling (Demske et al. 2005), which may be responsible for very low numbers of diatom valves counted from the Buguldeika Saddle (Prokopenko et al. 2007). Quantitative climate reconstructions indicate that pollen-inferred annual precipitation declined until almost 11 000 cal yrs BP, together with a significant decline in temperature of the coldest month (but little change in temperature of the warmest month) (Tarasov et al. 2007; 2009). In the catchment of Lake Baikal taiga forest was still present, although steppe and tundra biomes were widespread (Tarasov et al. 2007).

$\delta^{18}O_{modelled}$ record subsequently rises to its highest values (+35.6‰) at 10 750 cal yrs BP and remain above +30‰ until c. 10 305 cal yrs BP. These high values are coincident with both low %HSG (Fig 4) (Bond et al. 1997) and highest July insolation values (Prokopenko et al. 2007). Errors in the isotopic data however are also very high, most likely due to the very high levels of detected silt contamination (Fig 3). These data suggest that there must have been significant hydrological input into Lake Baikal during the early Holocene from rivers with southerly catchments. Independent evidence suggests that this is quite likely; pollen-inferred annual precipitation is very high at this time in southern Lake Baikal (between 500 – 600 mm/yr) (Tarasov et al. 2009), as are GCM modelled annual mean freshwater fluxes (cm/day) and JJA relative humidity (%) (Bush 2005). It is not clear if the high levels of contamination are a direct result of increased catchment in-wash, but diatom concentrations in several sites in the south basin of Lake Baikal are also very low at this time (e.g. Bradbury et al. 1994; Prokopenko et al. 2007) including the Vydrino shoulder (Morley 2005). Bradbury et al. (1994) suggest that periods of low diatom concentration may be related to a decline in water transparency caused by rivers bringing in terrigenous material, including fine clays and silts, depressing photosynthetic activity. While we are not yet in a position to confirm that this is the case, high levels of contamination (Fig 3) do not refute this hypothesis.

The greatest decline in the $\delta^{18}O_{modelled}$ record of +8‰ can be observed c. 10 275 – 10 030 cal yrs BP. This decline is synchronous with increased %HSG (IRD event no. 7) (Fig 4). This cool event is seen in several archives from the e.g. North Atlantic sediments and Greenland ice cores (c. 10 350 – 10 l50 cal yr BP: see Björck et al. 2001 for a synthesis). At this time, GCM modelled winter (DJF) temperatures showed a significant decline (data from Bush 2005 and Prokopenko et al. 2007), while a decline in an index of warm vegetation derived from Vydrino pollen confirms prevailing cooler conditions (Demske et al. 2005).

$\delta^{18}O_{modelled}$ shows an overall rise to relatively high values between c. 10 000 – 8 560 cal yrs BP. This isotopic increase occurs at the same time as a decline in %HSG (Fig 4), and an increase in abundances of vegetation in the catchment indicative of warm, moist climate (Demske et al. 2005; Tarasov et al. 2009). Thus, rivers such as the Selenga likely increased in importance at this time. Several North Atlantic regions show a cool event between c. 9 500 – 9 200 ka BP (IRD6), e.g. in Greenland ice cores (Rasmussen et al. 2007) and various European locations (e.g. von Grafenstein et al. 1999; McDermott et al. 2001), which Yu et al. (2010) attribute to freshwater outburst from Lake Superior in North America. There are minor fluctuations in the isotope data (e.g. at c. 9 645 cal yrs BP), which coincides with the start of increasing %HSG, but the decline at c. 9 200 cal yrs BP is not significant and well within variation of the isotope data themselves. Any impact of changes in the North Atlantic THC at this time on the composition of rivers flowing into Lake Baikal does not therefore appear to be as great as previous events, e.g. IRD 7 and 8).

There is a major decline in $\delta^{18}O_{modelled}$ record that starts c. 8 560 cal yrs BP, and reaches a minimum c. 8 400 cal yrs BP. This decline once again coincides with a peak in %HSG (Fig 4), IRD 5 (Bond et al. 2001). $\delta^{18}O_{modelled}$ values increase slightly again til c. 7 700 cal yrs BP, coinciding with a small decline in %HSG, before declining to a low value of 26.4‰ at c. 7 040 cal yrs BP, as %HSG increases to high abundances once more. Therefore, isotopic evidence suggests an increase in input into Lake Baikal from isotopically lower rivers with northern catchments, and a decline in rivers flowing in from the south between c. 8 560 – 7 040 cal yrs BP. Work on a Selenga River Holocene floodplain sequence at Burdukovo, which lies c. 30 km north of Ulan Ude, has revealed a switch from alluvial to aeolian sedimentation processes sometime between c. 8 180 – 7 725 cal yrs BP (White & Bush 2010). This also implies that Selenga River levels were low. Close inspection of other proxy records in the Lake Baikal region between c. 8 200 – 7 000 cal yrs BP show distinct low, modelled GCM summer temperatures (Bush 2005) together with marked drops in diatom abundances and biogenic silica (Prokopenko et al.

2007). Moreover, vegetation indicative of humid conditions also decline (ibid.) as does quantitative reconstruction of pollen-inferred annual precipitation (Tarasov et al. 2007), although these records are in contrast of GCM modeled summer humidity which increases at this time (Bush 2005).

Since 2001 a major international interdisciplinary programme (Baikal Archaeology Project) has sought to characterise cultural dynamics among hunter-gatherer populations around the Lake Baikal region during the mid Holocene (e.g. see Weber et al. 2002; 2010a). Results from this on-going research have redefined our understanding of hunter-gatherer adaptive strategies during the Neolithic–Bronze Age, including aspects of culture history, subsistence and diet, mobility patterns, genetic structure, and social and political relations. Most of these new archaeological data have been derived from numerous well-preserved formal cemetery contexts, which has allowed detailed analyses of human skeletal remains. Focus has especially centered around a distinct biocultural discontinuity between the early Neolithic Kitoi culture and the Serovo-Glazkovo cultures which inhabited the area during the late Neolithic – early Bronze Age (Weber et al. 2002). Thus by at least 7 000 cal yrs BP (i.e. middle Neolithic) there is a near absence of dated archaeological cemetery evidence in the cis-Baikal region (Weber et al. 2005, 2010b). In addition, clear shifts in subsistence adaptations (Katzenberg et al. 2010) and genetic affiliation (Mooder et al. 2006; 2010) are also identified between these pre- and post-hiatus groups. Reasons for this biological and cultural discontinuity are as yet uncertain, although several hypotheses have been put forward, including climate and environmental change (Weber et al. 2002; White and Bush 2010) and a decline in the use of formal cemeteries due to a shift in foraging behaviour (Weber et al. 2005). Tarasov et al. (2007) also reconstruct major changes in pollen-inferred climate variables between 7 200 – 6 000 cal yrs BP, most notably a decline in annual precipitation, concomitant with an increase in steppe vegetation. It is not possible at this stage to conclude whether or not this shift to a cooler, drier climate caused the observed hiatus between the Kitoi and Serovo-Glazkovo cultures, but climate influence ought not yet be discounted.

4.1.3 Mid – late Holocene (7 000 cal yrs BP – present)

Northern hemisphere summer insolation levels were still relatively high during the mid-Holocene, although North American ice sheets now had minimal impact on global climates (Mayewski et al. 2004; Wanner et al. 2008). Cool events associated with Bond cycles and increases in %HSG related to IRD4 to IRD0 were no longer associated with melt-water outbursts but likely caused by a combination of factors (see Wanner et al. 2008 for a review). During this period, $\delta^{18}O_{modelled}$ values exhibit different relationships the %HSG record in comparison to the similarities between the two records during the early Holocene. For example, as %HSG values increase after c. 7 000 cal yrs BP, $\delta^{18}O_{modelled}$ values also increase up to 5 890 cal yrs BP, at exactly the same time as increasing contamination, which suggests increased flow of rivers such as the Selenga and increased silt transport into the lake at the Vydrino site. This increase in $\delta^{18}O_{modelled}$ is also at odds with the decline in pollen-inferred precipitation between c. 7 200 – 6 000 cal yrs BP (Tarasov et al. 2007) and in water levels of the Mongolian lakes Hovsgol at c. 6 600 cal yrs BP (Dorofeyuk and Tarasov, 1998), and Telmen between c. 7 110 – 6 260 cal yrs BP (Peck et al. 2002). Further afield, a shift to heavier $\delta^{18}O$ values from Dongge Cave (south China) between 7 200 – 6 600 cal yrs BP highlights a weakening monsoon system, linked to strengthened Siberian High (Dykoski et al. 2005). There is a significant decline in $\delta^{18}O_{modelled}$ record between c. 5 980 and 5 600 cal yrs BP which is coincident with IRD4 and also with very low values for GCM modelled annual mean freshwater flux and JJA relative humidity (Bush 2005). Thus, while the inferred decline in fluvial input into Lake Baikal from southerly rivers at c. 5 700 cal yrs BP does coincide with weak North Atlantic thermohaline, increasing $\delta^{18}O_{modelled}$ values just prior to this event are at odds with other proxy records. More work therefore needs to be done to better characterise changes in precipitation and river inflow into Lake Baikal at this time.

After c. 5 165 cal yrs BP there is a sustained period of declining $\delta^{18}O_{modelled}$ values, which spans IRD3, leading to the low $\delta^{18}O_{modelled}$ value of 26.3‰ at c. 3 330 cal yrs BP, which coincides with IRD2 (Bond et al. 2001) (Fig. 4). The decline in $\delta^{18}O_{modelled}$ values coincides with variability observed in other regional proxy records, including a major phase of reconstructed steppe vegetation around Lake Baikal between c. 5 700 – 3 800 cal yrs BP (Tarasov et al. 2007). Diatom and biogenic silica profiles from the Buguldeika Saddle also show marked declines at this time, consistent with GCM data (Colman et al. 1999; Prokopenko et al. 2007). In northern Mongolia, low lake levels at Gun Nuur were recorded at c. 3 540 cal yrs BP (Dorofeyuk and Tarasov 1998). Together these proxies suggest a significant period of aridity, although other lakes, such as Telmen suggest more humid conditions prevailed after 4 390 cal yrs BP (Peck et al. 2002). In central China, $\delta^{18}O$ from Dongge Cave record the longest and one of the most significant periods of aridity during the Holocene (Wang et al. 2005) between c. 4 500 – 4 000 cal yrs BP. This period also coincides with IRD event 3 (Bond et al. 2001) and the collapse of the Neolithic culture in China.

From c. 3 330 - 2 630 cal yrs BP the $\delta^{18}O_{modelled}$ record is very poorly resolved. However, between c. 2 630 til c. 2 060 cal yrs BP, $\delta^{18}O_{modelled}$ values are at their highest during the mid- late Holocene, indicative of major influence of isotopically higher rivers flowing into Lake Baikal due to a weak Siberian High. High $\delta^{18}O_{modelled}$ values occur at the same time as low %HSG, very low steppe biome scores and increasing pollen-inferred temperatures (Tarasov et al. 2007). This increase is also mirrored by an increase in biogenic silica from the Buguldeika core (Prokopenko et al. 2007). Modelled annual freshwater flux also is very high at this time (Bush 2005). Regional records also concur with increased effective moisture. For example, in Lake Telmen laminated sediments accumulated between 2 210 and 2 070 cal yrs BP during which time deep lake levels must have predominated (Peck et al. 2002) due to high precipitation over northern Mongolia. Further south, proxy evidence from the Chinese Guliya ice cores highlight a period of marked warm and moist conditions, indicative of a weakened Siberian High and strong summer Asian monsoon (Yang et al. 2004). Proxy evidence from a number of different sources therefore confirm widespread warm and wet climate in the Lake Baikal region, coincidental with strengthened North Atlantic THC (Bond et al. 2001).

$\delta^{18}O_{modelled}$ record for the late Holocene is unfortunately at a very low resolution, making any useful comparisons to the %HSG record problematic. Overall, $\delta^{18}O_{modelled}$ values do decline towards the top of the record, coincident with declining biogenic silica concentrations (Prokopenko et al. 2007) and a marked fall in GCM modelled summer temperatures (Bush 2005). Low resolution $\delta^{18}O_{diatom}$ records from the north of Lake Baikal also decline at this time, highlighting the wide spatial extent of this event (Kalmychkov et al. 2007). A decline in effective moisture in northern Mongolia is also apparent in the sediment records from Lake Telmen, resulting in, for example, a high-stand terrace c. 1400 – 1260 cal yrs BP (Peck et al. 2002). Tree-ring data highlight a series of severe droughts affecting northern Mongolia during the early 18th and 19th centuries (Pederson et al. 2001). These observations are concurrent with the most recent IRD events in the North Atlantic, including event 0, which is coeval with the Little Ice Age. The drop in $\delta^{18}O_{diatom}$ values from c. 360 cal yrs BP might well be a response to a cooler climate associated with the LIA, which has been shown to have had a major impact on diatom communities close to Vydrino at this time (Mackay et a. 2005).

6. Conclusions

In this paper we present a new, recalculated mass-balanced model of $\delta^{18}O_{diatom}$ data for the late glacial – Holocene period in Lake Baikal. The improvement over a previous record has only been possible by accurately taking into account contaminants remaining in purified diatom silica samples, using electron optical imaging and whole sample geochemistry, as well as considering Al bound diatom concentrations. We interpret the $\delta^{18}O_{modelled}$ record as a proxy for the composition of river flow into Lake Baikal, with respect to the balance between rivers flowing into the lake with southern as opposed to northern catchments. Changes in this record show, in general, very good correspondence with proxy records of %HSG in the North Atlantic associated with enhanced meridional circulation at least during the early to mid Holocene. Between c. 7 000 – 6 000 cal yrs BP, increasing $\delta^{18}O_{modelled}$ values at odds with other proxy records in the region, and more work over this time frame needs to be undertaken to investigate possible reasons for this discrepancy.

7. Acknowledgements

Various funding sources have helped contribute to the production of data in this paper, including EU FPV *Continent* project (Contract EVK2-2000-00057); NERC NIGL (IP/635/0300); NERC PhD studentship to DWM (NER/S/A/2001/06430); Baikal Archaeology Project, supported by the Major Collaborative Research Initiative (MCRI) programme of the Social Sciences and Humanities Research Council of Canada; The Royal Society through the UK BICER programme.

8. References

Afanasjev AN. 1976. *The Water Resources and Water Balance of the Lake Baikal Basin* [in Russian]. Nauka, Novosibirsk.

Bezrukova EV, Abzaeva AA, Letunova PP, Kulagina NV, Vershin KE, Belov AV, Orlova LA, Danko LV, Krapivina SM. 2005. Post-glacial history of Siberian sprice (*Picea obovata*) in the Lake Baikal area and the significance of this species as a paleo-environmental indicator. *Quaternary International* **136 :** 47-57.

Björck S, Muscheler R, Kromer B, Andresen CS, Heinemeier J, Johnsen SJ, Conley D, Koç N, Spurk M, Veski S. 2001. High-resolution analyses of an early Holocene climate event may imply decreased solar forcing as an important climate trigger. *Geology* **29** : 1107-1110.

Blackwell, PG, Buck CE, Reimer PJ. 2006. Important features of the new radiocarbon calibration curves. *Quaternary Science Reviews* 25 **:** 408-413.

Bond G, Showers W, Cheseby M, Lotti R, Almasi P, deMenocal P, Priore P, Cullen H, Hajdas I, Bonani G. 1997. A pervasive millennial scale cycle in North Atlantic Holocene and glacial climates. *Science* **278** : 1257-1256.

Bond G, Kromer B, Beer J, Muscheler R, Evans M, Showers W, Hoffmann S, Lotti-Bond R, Hajdas I, Bonani G. 2001. Persistent solar influence on North Atlantic climate during the Holocene. *Science* **294** : 2130-2136.

Bradbury JP, Bezrukova YeV, Chernyaeva GP, Colman SM, Khursevich G, King JW, Likoshway YeV. 1994. A synthesis of post-glacial diatom records from Lake Baikal. *Journal of Paleolimnology* **10** : 213-252.

Brewer T, Leng M, Mackay AW, Lamb A, Tyler J, Marsh N. 2008. Unravelling contamination signals in biogenic silica oxygen isotope composition: the role of major and trace element geochemistry. *Journal of Quaternary Science* **23** : 365-374.

Bronk Ramsey C. 2009. Bayesian analysis of radiocarbon dates. *Radiocarbon* **51** : 337-360.

Bush ABG. 2005. CO_2/H_2O and orbitally driven climate variability over central Asia through the Holocene. *Quaternary International* **136** : 15-23.

Campbell ID, Campbell C, Apps M, Rutter NW, Bush ABG. 1998. Late Holocene ~1500 yr climatic periodicities and their implications. *Geology* **26** : 471-473.

Charlet F. Fagel N, De Batist M, Hauregard F, Minnebo B, Meischner D, SONIC Team. 2005. Sedimentary dynamics on isolated highs in Lake Baikal: evidence from detailed high-resolution geophysical data and sediment cores. *Global and Planetary Change* **46** : 125-144.

Chebykin EP, Edgington DN, Grachev MA, Zzheleznyakova TO, Vorobyova SS, Kulikova NS, Azarova IN, Khlystov OM, Goldberg EL. 2002. Abrupt increase in precipitation and weathering of soils in East Siberia coincident with the end of the last glaciation (15 cal kyr BP). *Earth and Planetary Science Letters* **200** : 167-175.

Colman SM, Peck JA, Hatton J, Karabanov EB, King JW. 1999. Biogenic silica records from the BDP93 drill site and adjacent areas of the Selenga Delta, Lake Baikal, Siberia. *Journal of Paleolimnology* **21** : 9-17.

deMenocal P, Oritz J, Guilderson T, Sarnthein M. 2000. Coherent high and low latitude climate variability during the Holocene warm period. *Science* **288** : 2198-2202.

Demske D, Heumann G, Granoszewski W, Nita M, Mamakowa K, Tarasov PE, Oberhänsli H. 2005. Late glacial and Holocene vegetation and regional climate variability evidenced in high-resolution pollen records from Lake Baikal. *Global & Planetary Change* **46** : 255-279.

Dorofeyuk NI, Tarasov PE. 1998. Vegetation and lake leves in northern Mongolia during the past 12500 years from palynological and diatom analyses. *Stratigraphy and Geologic Correlation* **6** : 73-87.

Dykoski CA, Edwards RL, Cheng H, Yuan D, Cai Y, Zhang M, Lin Y, Qing J, An Z, Revenaugh J. 2005. A high-resolution, absolute-dated Holocene and deglacial Asian monsoon record from Dongge Cave, China. *Earth and Planetary Science Letters* **233** : 71-86.

Fisher TG, Smith DG, Andrews JT. 2002. Preboreal oscillation caused by a glacial Lake Agassiz flood. *Quaternary Science Reviews* **21** : 873-878.

Grunert J, Lehmkuhl F, Walther M. 2000. Paleoclimatic evolution of the Uvs Nuur basin and adjacent areas (Western Mongolia). *Quaternary International* **65-66** : 171-192.

Hampton SE, Izmest'eva LR, Moore MV, Katz SL, Dennis B, Silow EA. 2008. Sixty years of environmental change in the world's largest freshwater lake–lake Baikal, Siberia. *Global Change Biology* **14** : 1947-1958.

Heegaard E, Birks HJB, Telford RJ. 2005. Relationships between calibrated ages and depth in stratigraphical sequences: as estimation procedure by mixed-effect regression. *The Holocene* **15** : 612-618.

Heiri O, Tinner W, Lotter A. 2004. Evidence for cooler European summers during periods of changing meltwater flux to the North Atlantic. *Proceedings of the National Academy of Sciences* **101** : 15285-15288.

Hu, FS, Shemesh A. 2003. A biogenic-silica $\delta^{18}O$ record of climatic change during the last glacial-interglacial transition in southwestern Alaska. *Quaternary Research* **59** : 379-385.

Jones VJ, Leng MJ, Solovieva N, Sloane H, Tarasov P. 2004. Holocene climate of the Kola Peninsula; evidence from the oxygen isotope record of diatom silica. *Quaternary Science Reviews* **23** : 833-839.

Kalmychkov GV, Kuzmin MI, Pokrovskii BG, Kostrova SS. 2007. Oxygen isotopic composition in diatom algae frustules from Lake Baikal sediments: annual mean temperature variations during the last 40 ka. *Doklady Earth Sciences* **413** : 206-209.

Katzenberg MA, Bazaliiskii VI, Goriunova OI, Savel'ev NA, Weber AW. 2010. Diet reconstruction and stable isotope ecology in the Lake Baikal region. In *Prehistoric Hunter-Gatherers of the Baikal Region, Siberia: Bioarchaeological Studies of Past Lifeways*, Weber AW, Katzenberg MA, Schurr TG (eds) University of Pennsylvania Museum Press. in press.

Koning E, Gehlen M, Flank AM, Calas G, Epping E. 2007. Rapid post-mortem incorporation of aluminum in diatom frustules: evidence from chemical and structural analyses. *Marine Chemistry* **103** : 97–111.

Kozhova OM, Izmest'eva LR. 1998. *Lake Baikal: evolution and biodiversity*. Backhuys Publishers: Leiden.

Kurita N, Yoshida N, Inoue G, Chayanova EA. 2004. Modern isotope climatology of Russia: a first assessment. *Journal of Geophysical Research* **109** : D03102 15 pp.

Lamb AL, Brewer TS, Leng MJ, Sloane HJ, Lamb HF. 2007. A geochemical method for removing the effect of tephra on lake diatom oxygen isotope records. *Journal of Paleolimnology* **37** : 499-516.

Leng M, Barker P. 2006. A review of the oxygen isotope composition of lacustrine diatom silica. *Earth Science Reviews* **75** : 5-27.

Leng MJ, Sloane H. 2008. Combined oxygen and silicon isotope analysis of biogenic silica. *Journal of Quaternary Science* **23** : 3113-319.

Livingstone DM. 1999. Ice break-up on southern Lake Baikal and its relationship to local and regional air temperatures in Siberia and to the North Atlantic Oscillation. *Limnology & Oceanography* **44** : 1486-1497.

Lui X, Yanai M. 2002. Influence of Eurasian spring snow cover on Asian summer rainfall. *International Journal of Climatology* **22** : 1075-1089.

Lydolph PE. 1977. *Eastern Siberia*. In *Climates of the Soviet Union. World Survey of Climatology*, **7**, Elsevier, pp 91-115.

Ma X, Yasunari T, Ohata T, Natsagdorj L, Davaa G, Oyunbaatar D. 2003. Hydrological regime analysis of the Selenge River basin, Mongolia. *Hydrological Processes* **17** : 2929-2945.

Mackay AW, Ryves DB, Battarbee RW, Flower RJ, Jewson D, Rioual PMJ, Sturm M. 2005. 1000 years of climate variability in central Asia: assessing the evidence using Lake Baikal diatom assemblages and the application of a diatom-inferred model of snow thickness. *Global & Planetary Change* **46** : 281-297.

Mackay AW, Karabanov E, Khursevich G, Leng M, Morley DW, Panizzo VN, Sloane HJ, Williams D. 2008. Reconstructing hydrological variability in Lake Baikal during MIS 11: an application of oxygen isotope analysis of diatom silica. *Journal of Quaternary Science* **23** : 365-374.

Mayewski PA, Rohling EE, Stager JC, Karlén W, Maasch KA, Meeker LD, Meyerson EA, Gasse F, van Kreveld S, Holmgren K, Lee-Thorp J, Rosqvist G, Rack F, Staubwasser M, Schneider RR, Steig EJ. 2004. Holocene climate variability. *Quaternary Research* **62** : 243-255.

McDermott F, Mattey DP, Hawkesworth CJ. 2001. Centennial scale Holocene climate variability revealed by a high-resolution speleothems ^{18}O record from S. W. Ireland. *Science* **294** : 1328.

Mooder KP, Schurr TG, Bamforth FJ, Bazaliiski VI, Savel'ev NA. 2006. Population affinities of Neolithic Siberians: a snapshot from prehistoric Lake Baikal. *American Journal of Physical Anthropology* **129** : 349–61.

Mooder KP, Thomson TA, Weber AW, Bazaliiskii VI, Bamforth F. 2010. Uncovering the genetic landscape of prehistoric Cis-Baikal. In *Prehistoric Hunter-Gatherers of the Baikal Region, Siberia: Bioarchaeological Studies of Past Lifeways*, Weber AW, Katzenberg MA, Schurr TG (eds) University of Pennsylvania Museum Press. 107-120.

Morley DW. 2005. *Reconstructing past climate variability in continental Eurasia*. Unpublished PhD Thesis, University of London.

Morley DW, Leng MJ, Mackay AW, Sloane H, Rioual P, Battarbee RW. 2004. Cleaning of lake sediment samples for diatom oxygen isotope analysis. *Journal of Paleolimnology* **31** : 391-401.

Morley DW, Leng MJ, Mackay AW, Sloane HJ. 2005. Late Glacial and Holocene atmospheric circulation change in the Lake Baikal region documented by oxygen isotopes from diatom biogenic silica. *Global & Planetary Change* **46** : 221-233.

Murton JB, Bateman MD, Dallimore SR, Teller JT, Yang Z. 2010. Identification of Younger Dryas outburst flood path from Lake Agassiz to the Arctic Ocean. *Nature* **464** : 740-743.

Nesje A, Jansen E, Birks HJB, Bjune AE, Bakke J, Andersson C, Dahl SO, Kristensen DK, Lauritzen S-E, Lie Ø, Risebrobakken B, Svendsen I. 2005. Holocene climate variability in the northern North Atlantic region: a review of terrestrial and marine evidence. In: *The Nordic Seas: An integrated perspective*, *Geophysical Monograph Series* **158** : 289-322.

Numaguti A. 1999. Origin and recycling processes of precipitating water over the Eurasian continent: experiments using an atmospheric general circulation model. *Journal of Geophysical Research* **104** : 1957-1972.

Peck JA, Khosbayar P, Fowell SJ, Pearce RB, Ariunbileg S, Hansen BCS, Soninkhishig N. 2002. Mid to Late Holocene climate change in north central Mongolia as recorded in the sediments of Lake Telmen. *Palaeogeography, Palaeoclimatology, Palaeoecology* **183** : 135-153.

Pederson N, Jacoby GC, D'Arrigo RD, Cook ER, Buckley BM. 2001. Hydrometerological reconstructions for northeastern Mongolia derived from tree rings: 1651-1995. *Journal of Climate* **14** : 872-881.

Piotrowska N, Bluszcz A, Demske D, Granoszewski W, Heumann G. 2004. Extraction and AMS radiocarbon dating of pollen from Lake Baikal sediments. *Radiocarbon* **46** : 181-187.

Prokopenko AA, Kuzmin MI, Williams DF, Gelety VF, Kalmychkov GV, Gvozdkov AN, Solotchin PA. 2005. Basin-wide sedimentation changes and deglacial lake-level rise in the Hovsgol basin, NW Mongolia. *Quaternary International* **136** : 59-69.

Prokopenko AA, Khursevich GK, Bezrukova EV, Kuzmin MI, Boes X, Williams DF, Fedenya SA, Kulagina NV, Letunova PP, Abzaeva AA. 2007. Paleoenvironmental proxy records from Lake Hovsgol, Mongolia, and a synthesis of Holocene climate change in the Lake Baikal watershed**.** *Quaternary Research* **68** : 2-17.

Prokopenko AA, Kuzmin MI, Li H-C, Woo K-S, Catto NR. 2009. Lake Hovsgol basin as a new study site for long continental paleoclimate records in continental interior Asia: general context and current status. *Quaternary International* **205** : 1-11.

Rasmussen DO, Andersen KK, Svensson AM, Steffensen JP, Vinther BM, Clausen HB, Siggaard-Andersen M-L, Johnsen SJ, Larsen LB, Dahl-Jensen D, Bigler M, Rothlisberger R, Fischer H, Goto-Azuma K, Hansson ME, Ruth U. 2006. A new Greenland ice core chronology for the last glacial termination. *Journal of Geophysical Research* **111** : 1 of 16.

Rasmussen SO, Vinther BM, Clausen HB, Andersen KK. 2007. Early Holocene climate oscillations recorded in three Greenland ice cores. *Quaternary Science Reviews* **26** : 1907–14.

Reimer PJ, Baillie MGL, Bard E, Bayliss A, Beck JW, Bertrand CJH, Blackwell PG, Buck CE, Burr GS, Cutler KB, Damon PE, Edwards RL, Fairbanks RG, Friedrich M, Guilderson TP, Hogg AG, Hughen KA, Kromer B, McCormac G, Manning S, Ramsey CB, Reimer RW, Remmele S, Southon JR, Stuiver M, Talamo S, Taylor FW, Van der Plicht J, Weyhenmeyer CE. 2004. IntCal04 Terrestrial Radiocarbon Age Calibration, 0–26 Cal Kyr BP. *Radiocarbon* **46** : 1029-1058.

Rosqvist G, Jonsson C, Yam R, Karlén W, Shemesh A. 2004. Diatom oxygen isotopes in pro-glacial lake sediments from northern Sweden: a 5000 year record of atmospheric circulation. *Quaternary Science Reviews* **23** : 851-859.

Sato T, Tsujimura M, Yamanaka T, Iwasaki H, Sugimoto A, Sugita M, Kimura F, Davaa G, Oyunbaatar D. 2007. Water sources in semi-arid Northeast Asia as revealed by field observations and isotope transport model. *Journal of Geophysical Research- Atmospheres* **112** : D17112.

Seal RR, Shanks WC. 1998. Oxygen and hydrogen isotope systematics of Lake Baikal, Siberia: implications for palaeoclimate studies. *Limnology & Oceanography* **43** : 1251-1261.

Shemesh A, Rosqvist G, Rietti-Shati M, Rubensdotter L, Bigler C, Yam R, Karlén W. 2001. Holocene climatic change in Swedish Lapland inferred from an oxygen-isotope record of lacustrine biogenic silica. *The Holocene* **11** : 447-454.

Shimaraev MN, Verbolov VI, Granin NG, Sherstyankin PP. 1994. *Physical limnology of Lake Baikal: a review.* BICER : Irkutsk-Okayama.

Soma Y, Tani Y, Soma M, Mitake H, Kurihara R, Hashomoto S, Watanabe T, Nakamura T. 2007. Sedimentary steryl chlorin esters (SCEs) and other photosynthetic pigments as indicators of palaeolimnological change over the last 28,000 years from the Buguldeika Saddle of Lake Baikal. *Journal of Paleolimnology* **37** : 163-175.

Stuiver M, Grootes PM, Braziunas TF. 1995. The GISP2 $\delta^{18}O$ climatic record of the past 16,500 years and the role of the sun, ocean, and volcanoes. *Quaternary Research* **44** : 341–354.

Swann GEA. in press. A comparison of the Si/Al and Si/time wet-alkaline digestion methods for measurement of biogenic silica in lake sediments. *Journal of Paleolimnology*

Swann GEA, Leng MJ. 2009. A review of diatom ^{18}O in palaeoceanography. *Quaternary Science Reviews* **28** : 384-398.

Tarasov L, Peltier WR. 2005. Arctic freshwater forcing of the Younger Dryas cold reversal. *Nature* **435** : 662-665.

Tarasov P, Bezrukova E, Karabanov E, Nakagawa T, Wagner M, Kulagina N, Letunova P, Abzaeva A, Granoswewski W, Riedal F. 2007. Vegetation and climate dynamics during the Holocene and Eemian interglacials derived from Lake Baikal pollen records. *Palaeogeography, Palaeoclimatology, Palaeoecology* **252** : 440-457.

Tarasov PE, Bezrukova EV, Krivonogov SK. 2009. Late Glacial and Holocene changes in vegetation cover and climate in southern Siberia derived from a 15 kyr long pollen record from Lake Kotokel. *Climate of the Past Discussions* **5** : 127-151.

Todd MC, Mackay AW. 2003. Large-scale climate controls on Lake Baikal ice cover. *Journal of Climate* **16** : 3186-3199.

von Grafenstein U, Erlenkeuser H, Brauer A, Jouzel J, Johnsen SJ. 1999. A mid-European decadal isotope-climate record from 15,500 to 5000 years BP. *Science* **284** : 1654– 1657.

Wang Y, Cheng H, Edwards RL, He Y, Kong X, An Z, Wu J, Kelly MJ, Dykoski CA, Li X. 2005. The Holocene Asian monsoon: links to solar changes and North Atlantic climate. *Science* **308** : 854-857.

Wanner H, Beer J, Bütikofer J, Crowley TJ, Cubasch U, Flückiger J, Goosse H, Grosjean M, Joos F, Kaplan JO, Küttel M, Müller SA, Prentice C, Solomina O, Stocker TF, Tarasov P, Wagner M, Widmann M. 2008. Mid- to Late Holocene climate change: an overview. *Quaternary Science Reviews* **27** : 1791-1828.

Watanabe T, Nakamura T, Watanabe Nara F, Kakegawa T, Nishimura M, Shimokawara M, Matsunaka T, Senda R, Kawai T. 2009. A new age model for the sediment cores from Academician ridge (Lake Baikal) based on high-time-resolution AMS ^{14}C data sets over the last 30 kyr: paleoclimatic and environmental implications. *Earth and Planetary Science Letters* **286** : 347-354.

Weber AW, Link DW, Katzenberg MA. 2002. Hunter-gather culture change and continuity in the middle Holocene of the cis-Baikal, Siberia. *Journal of Anthropological Archaeology* **21** : 230-299.

Weber AW, McKenzie HG, Beukens R. 2005. Evaluation of radiocarbon dates from a Middle Holocene hunter-gatherer cemetery Khuzhir-Nuge XIV, Lake Baikal, Siberia. *Journal of Archaeological Science* **32** : 1481–1500.

Weber AW, Katzenberg MA, Schurr TG. Eds. 2010a. *Prehistoric Hunter-Gatherers of the Baikal Region, Siberia: Bioarchaeological Studies of Past Lifeways*. Pp xv-xx.

Weber AW, McKenzie HG, Beukens R. 2010b. Radiocarbon dating of Middle Holocene culture history in the Cis-Baikal. In *Prehistoric Hunter-Gatherers of the Baikal Region,* *Siberia: Bioarchaeological Studies of Past Lifeways*, Weber AW, Katzenberg MA, Schurr TG (eds) University of Pennsylvania Museum Press. 27-50.

White D, Bush ABG. 2010. Holocene climate, environmental variability and Neolithic biocultural discontinuity in the Lake Baikal region. In *Prehistoric Hunter-Gatherers of the Baikal Region, Siberia: Bioarchaeological Studies of Past Lifeways*, Weber AW, Katzenberg MA, Schurr TG (eds) University of Pennsylvania Museum Press. 1-26.

Yang B, Braeuning A, Shi Y, Chen F. 2004. Evidence for a late Holocene warm and humid climate period and environmental characteristics in the arid zones of northwest China during 2.2 ~ 1.8 kyr BP. *Journal of Geophysical Research* **109** : D02105.

Yu S-Y, Colman SM, Lowell TV, Milne GA, Fisher TG, Breckenridge A, Boyd M, Teller JT. 2010. Freshwater outburst from Lake Superior as a trigger for the cold event 9300 years ago. *Science* **328** : 1262-1266.

Figure legends

Fig. 1. Location of Lake Baikal, its three largest tributaries (Selenga, Upper Angara and Barguzin rivers), its outflow (Angara River) and coring location at the Vydrino Shoulder.

Fig. 2. Age-depth model based on calibrated radiocarbon AMS dates for composite cores from Vydrino Shoulder (CON01-605-5 and CON01-605-3) constructed using a generalised mixed-effect regression based on a generalised additive model (GAM) with constant variance (Heegaard et al. 2005). Grey-shaded area represents 95% confidence intervals of modelled ages (black line), black diamonds – midpoints of calibrated age ranges.

Fig 3. Comparative plots showing $\delta^{18}O_{diatom}$ (open circles) (Morley et al. 2005) and $\delta^{18}O_{modelled}$ (closed black squares; this study) profiles. % silt contamination is calculated from the amount of Al_2O_3 in individual samples. See text for details.

Fig. 4. Stratigraphic profiles of proxies highlighted in the text, plotted on a radiocarbon calibrated age scale. $\delta^{18}O_{modelled}$ profile with associated errors linked to mass-balancing isotope measurements (see text for details); four stacked records of relative abundance of hematite stained grains (%HSG) in North Atlantic sediments indicative of ice rafted debris events (see Bond et al. 2001 for full details). IRD numbers are according to those originally given in Bond et al. (1997). YD (Younger Dryas) and IACP (intra-Allerød cold period) are also highlighted.

Table 1. Sediment cores collected from the Vydrino Shoulder, Lake Baikal

Core code	Type	Lat.	Long.	Water depth	Core length
CON01-605-3	piston	51.5849	104.8548	675 m	10.45 m
CON01-605-5	box	51.5835	104.8518	665 m	2.50 m

Table 2. Radiocarbon dating profile from Vydrino location in the south basin of Lake Baikal. AMS dates from pollen extracts were calibrated using Oxcal4.1 program and IntCal04 radiocarbon calibration curve (Reimer et al. 2004). Depth interval and mid-depth are the original depths of samples from either the box core (CON01-605-5) or the piston core (CON01-605-3); sample thickness is the thickness of sediment samples processed to obtain pollen and spore concentrates; corrected depth values are those determined once cores have been spliced together and missing core tops taken into account; pollen purity (%) was estimated on the basis of particle counts; age ^{14}C BP are uncalibrated radiocarbon ages; unc is the laboratory uncertainty associated with each ^{14}C age; calibrated age range is limited by younger and older boundaries for 95.4% probability distribution of calendar age obtained after calibration; mid-point 94.5% is the central point estimation of the calibrated age range, and +/- is half of this range.

Table 3. Comparison of summary $\delta^{18}O$ between datasets presented by Morley et al. (2005) and this study.

	Lowest (‰)	**highest (‰)**	**range (‰)**	**mean (‰)**	**No of samples**
Morley et al. (2005)	14.4	29.4	15.0	23.6 +/- 3.82	130
This study	23.9	35.6	11.7	28.7 +/- 2.15	55

Table 2

Core	Core code	Depth interval		Mid-depth	Sample thickness, cm	Corrected depth, cm	Pollen purity (%)	Age ^{14}C BP	unc	Calibrated ag range, 95.4 probability	
Box	LBB-AMS-1	0	4	2	4	14.5	90	1950	35	1950	17
Box	LBB-AMS-2	20	24	22	4	34.5	95	2375	25	2680	23
Box	LBB-AMS-3	32	35	33.5	3	46	95	2945	30	3215	30
Box	LBB-AMS-4	56	59	57.5	3	70	95	4530	40	5310	50
Box	LBB-AMS-5	77	80	78.5	3	91	95	5455	35	6305	62
Box	LBB-AMS-6	89	92	90.5	3	103	90	6170	40	7160	69
Box	LBB-AMS-7	101	104	102.5	3	115	85	6700	40	7650	75
Box	LBB-AMS-8	121	124	122.5	3	135	85	7760	40	8605	84
Box	LBB-AMS-9	138	141	139.5	3	152	90	8620	40	9680	95
Piston	LBF-AMS-11a	12	18	15	6	154	n.d.	8810	50	9840	95
Box	LBB-AMS-10	145	148	146.5	3	159	90	8750	50	10120	97
Box	LBB-AMS-11	159	163	161	4	173.5	90	9470	50	11060	105
Box	LBB-AMS-12	171.5	175.5	173.5	4	186	80	10030	50	11810	113
Piston	LBF-AMS-12a	48	56	52	8	191	n.d.	10340	60	12230	118
Piston	LBF-AMS-13	65	73	69	8	208	n.d.	10730	60	12850	126
Piston	LBF-AMS-14	90	98	94	8	233	n.d.	11820	70	13890	135
Piston	LBF-AMS-15	116	124	120	8	259	n.d.	13340	130	16090	152

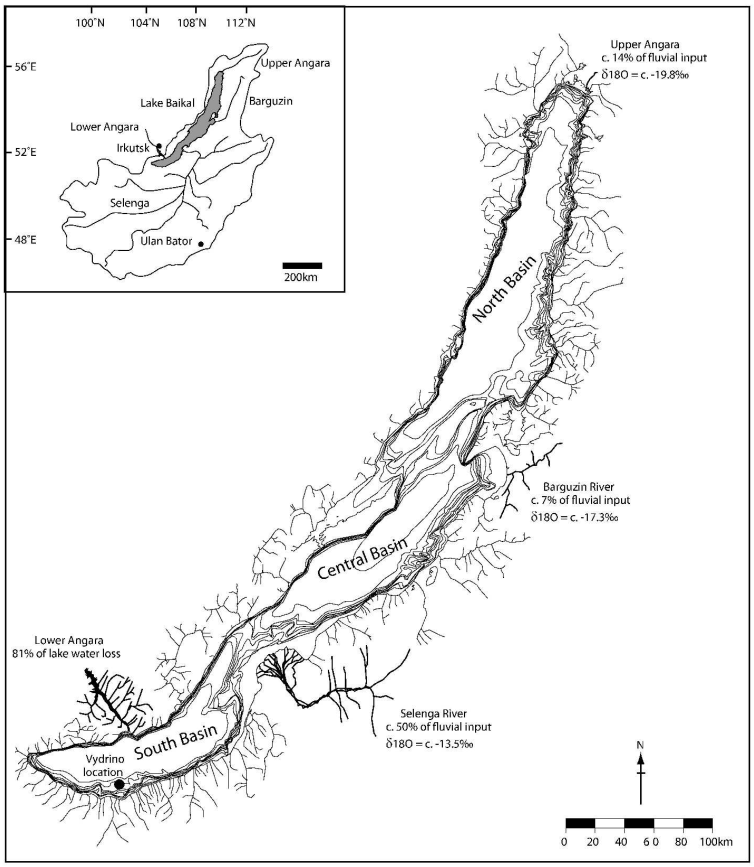

Location of Lake Baikal, its three largest tributaries (Selenga, Upper Angara and Barguzin rivers), its outflow (Angara River) and coring location at the Vydrino Shoulder.
201x288mm (600 x 600 DPI)

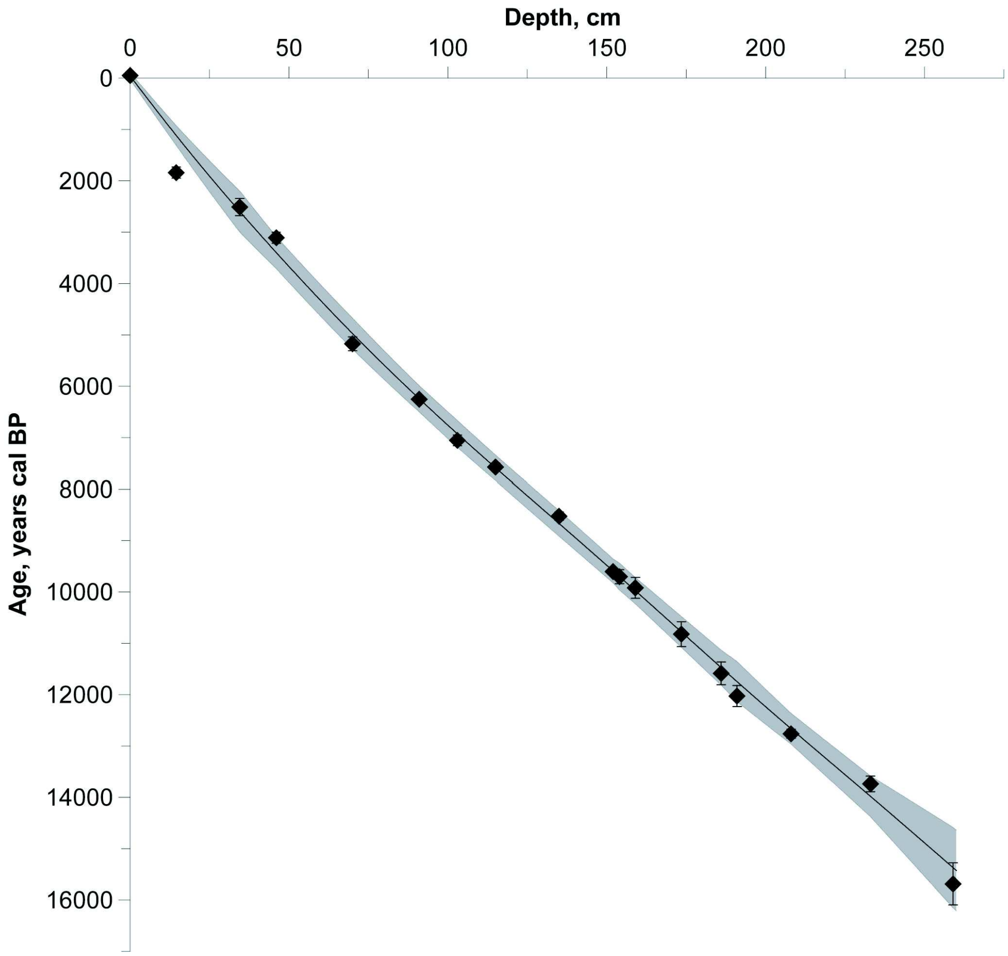

Age-depth model based on calibrated radiocarbon AMS dates for composite cores from Vydrino Shoulder (CON01-605-5 and CON01-605-3) constructed using a generalised mixed-effect regression based on a generalised additive model (GAM) with constant variance (Heegaard et al. 2005). Grey-shaded area represents 95% confidence intervals of modelled ages (black line), black diamonds – midpoints of calibrated age ranges
174x165mm (600 x 600 DPI)

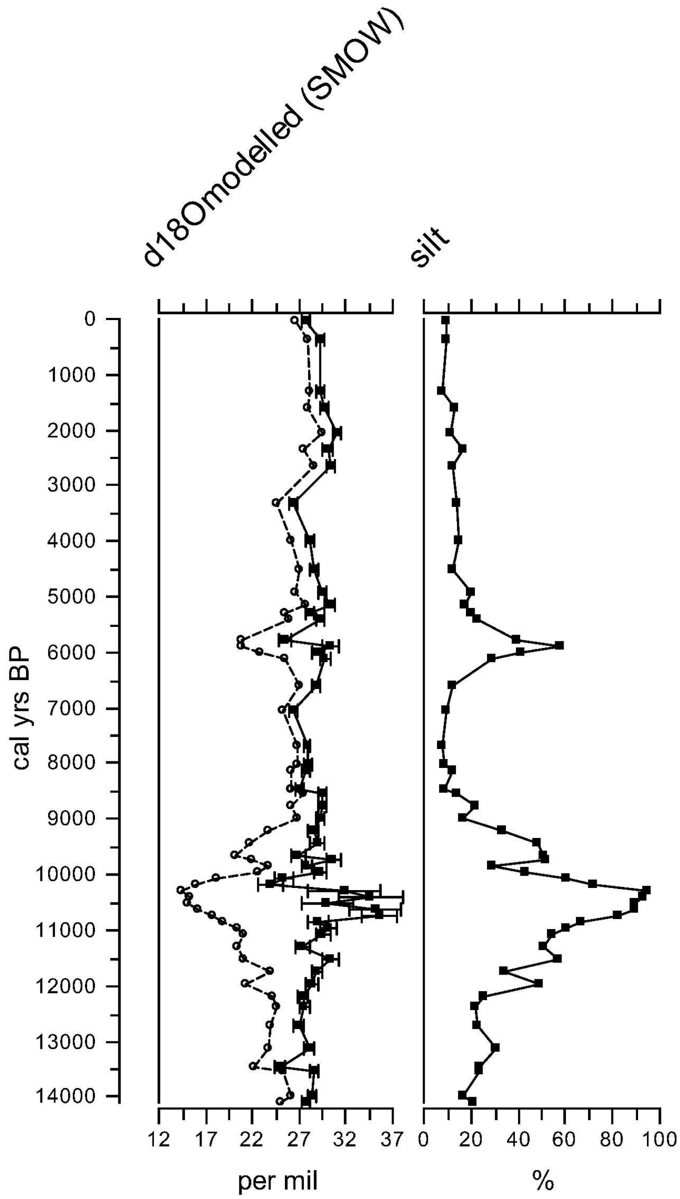

Comparative plots showing δ18Odiatom (open circles) (Morley et al. 2005) and δ18Omodelled (closed black squares; this study) profiles. % silt contamination is calculated from the amount of Al2O3 in individual samples. See text for details.
108x192mm (600 x 600 DPI)

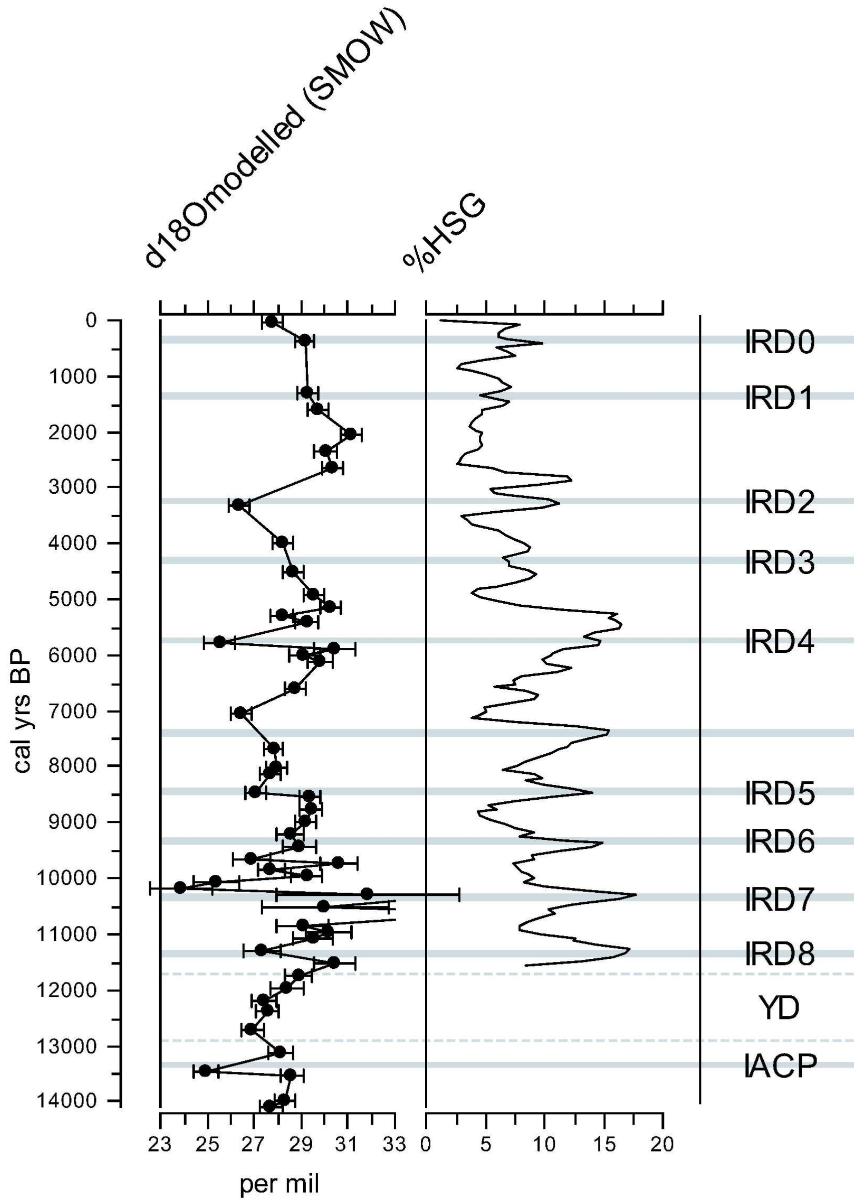

Stratigraphic profiles of proxies highlighted in the text, plotted on a radiocarbon calibrated age scale. δ18Omodelled profile with associated errors linked to mass-balancing isotope measurements (see text for details); four stacked records of relative abundance of hematite stained grains (%HSG) in North Atlantic sediments indicative of ice rafted debris events (see Bond et al. 2001 for full details). IRD numbers are according to those originally given in Bond et al. (1997). YD (Younger Dryas) and IACP (intra-Allerød cold period) are also highlighted.
136x192mm (600 x 600 DPI)